

## Downward Continuation of Common Midpoint Gathers By Transformation into Snell Trace Coordinates

*Rick Ottolini*

### Abstract

This report studies a gather-only subset of the theory developed by Ottolini in "Migration of Radial Trace Sections" (SEP-20). First, Snell trace coordinates are distinguished from radial trace coordinates as incorporating a depth variable velocity structure. Next, the downward continuation algorithm is shown to be a  $p$ -dependent time shift in Snell trace coordinates. Finally, synthetic and real data examples demonstrate the workability of this method. These examples are compared to radial trace and the wave-equation based phase shift downward continuation methods. The Snell trace coordinate method has fewer artifacts than the wave equation scheme.

### Definition of the Snell Trace

Both the *radial trace* and *Snell trace* are mappings of a common midpoint gather along diagonal trajectory passing through the origin. The trajectory of radial trace is straight, while the Snell trace may be curved as shown in figure 1. The name *Snell trace* derives from that its trajectory is a function of a stratified earth velocity model  $v(z)$  and the Snell parameter  $p$ .

The trajectory of a Snell trace mapping is determined according to the geometry in figure 2. It is the line formed by the set of tangency points of a linear moveout coordinate system with flat-earth moveout hyperbolas for every zero offset depth. As proved in previous SEP articles (Claerbout SEP-15:81), the slant angle of a linear moveout coordinate system is the Snell parameter. From the derivations in Ottolini's SEP-20 report, the trajectory of a Snell trace in a stratified earth is given by

$$h_S = \int_0^z dz \tan \vartheta(z) \quad (1)$$

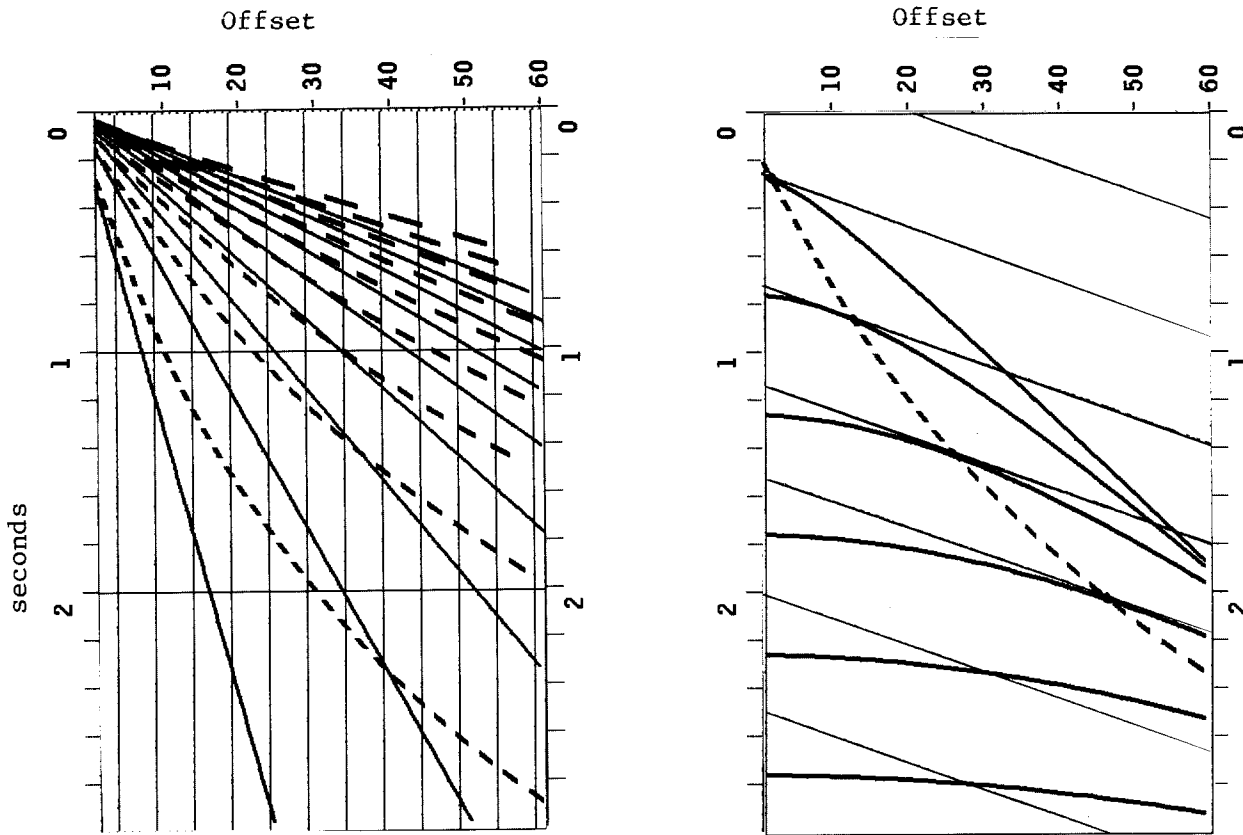


FIG. 1. This figure displays the difference between Snell trace trajectories (curved dashed lines) and radial trace trajectories (straight solid lines). Both sets of lines are computed for the same range of Snell parameters but different depth velocity profiles. The velocity used for the Snell trace trajectories is taken from the Conoco data example in Clayton et al (this report). The trajectories curve upward because velocity increases with depth. The velocity used for the radial trace trajectories is the water velocity. Other parameters include #offsets=60 near=.162km  $\Delta\text{off}=.05\text{km}$  #t=750  $\Delta t=.004\text{s}$  tfinal=3sec #p=10 firstp=0.  $\Delta p=.04\text{s/km}$ .

FIG. 2. Snell trace trajectories are determined from the geometry shown in this figure. The Snell trace trajectory (dashed line) is the set of tangency points of a linear moveout coordinate system (slanted solid lines) with flat-earth moveout hyperbolas (curved solid lines) for every zero offset depth. The parameters are the same as in figure 1. The Snell parameter of the linear moveout and Snell trace trajectories is .06km/s.

$$t_S = \int_0^z dz \frac{v(z)}{\cos\vartheta(z)} \quad (2)$$

where the  $S$  subscripts stand for the trajectory intercepts. The angles are shorthand for the Snell parameter relation  $\sin\vartheta(z) = v(z)p$ . In a constant velocity earth equations (1) and (2) reduce to the equation of a straight line

$$h_S = pv^2 t_S \quad (3)$$

which is the same as a radial trace mapping.

The assumptions made in this derivation are (1) a flat earth and (2) events have only one velocity for a given travelttime. The second assumption constrains the use of Snell traces in datasets with multiples.

We can establish the following ranking for various coordinate systems which use the Snell parameter.

<i>Coordinates</i>	<i>Velocity</i>	<i>Name</i>
h t y		common midpoint gathers and constant offset sections
p t y	$\bar{v}$	radial trace gathers and sections
p t y	$v(z)$	Snell trace gathers and sections
p t y	$v(z)$	slant stack gathers and sections

Gathers refer to a set of traces with a fixed midpoint and the Snell parameter (or offset) that increases from trace to trace. Sections are a set of traces with a fixed Snell parameter (or offset) and the midpoint changes from trace to trace.

We may make general comparisons between these four coordinate systems based upon the previous SEP research of Ottolini, Claerbout, and Yilmaz and articles in this SEP report. From a theoretic standpoint, the most satisfactory coordinate system do imaging in is the slant stack coordinate system, and the least satisfactory is the midpoint-offset coordinate system. Operations on common midpoint gathers or constant offset sections run into problems of dip and top-flattened hyperbolas. The operators in slant stack coordinates are mathematically exact, but good slant stacks are difficult to construct. Snell and radial trace coordinates are approximations to slant stack coordinate which have some of the mathematical advantages of slant stack coordinates and are easier to transform into than slant stacks. As this report will show, Snell trace coordinates are more suitable for downward continuation in a stratified velocity media than radial trace coordinates.

Snell and radial trace coordinates can be used for seismic data processing other than imaging. Gonzalez and Claerbout (this SEP volume) show that deforming Snell trace gathers

into radial trace gathers aids velocity analysis. Morley (this SEP volume) shows that radial trace coordinates can be used to detect and eliminate multiple reflections.

### **Downward Continuation Algorithm**

The downward continuation of a Snell trace gather is simply a  $p$ -dependent shift of each trace. The following two-step proof of this assertion leads to a formula for this shift. First, it was shown in the SEP-20 article there is an equation which maps Snell traces into slant stack coordinates and visa-versa. The transformation itself is only a depth variable time shift. The equation is not repeated here because it is not necessary for computing how to downward continue Snell traces.

The second part of the proof is that the downward continuation of slant stack gathers is also merely a  $p$ -dependent time shift. It was derived by Clayton and McMechan in SEP-24 and is repeated in the appendix. Given the depth one wishes to downward continue a slant stack gather, the amount of the time shift is the time at which a hypothetical event for that downward continuation depth would appear on each slant stack trace. This equivalent to the interpretation made by Schultz [1], that in order to downward continue to a certain reflector, the shape of the reflector is flattened on a slant stack gather, and the events above it shaved off.

A algorithm for downward continuing Snell traces is obtained by combining both parts of this proof. Since a Snell trace is just a time stretch of a slant stack trace, a Snell trace gather may be downward continued by shaving off all of the gather above a hypothetical event occurring at the downward continuation depth. The amount of the time shift is computed by equation (2) where the  $z$  bound of the integral is the downward continuation depth.

The downward continuation of a CDP gather is done in three stages. First map a CDP gather into a Snell trace gather. Snell traces are extracted using equations (1) and (2). From experience, the number of Snell parameters show be comparable to the number of offsets in a gather. The Snell parameters should be evenly distributed between the steepest and shallowest time dips present on the CDP gather. Second, apply a time shift given by equation (2) where  $z$  is the downward continuation depth to each trace of the Snell trace gather. Finally, inverse map back into a common midpoint gather.

The three stages of this algorithm are illustrated in figures 3 through 6.

### Data Examples and Evaluation

Synthetic and field data are used to demonstrate:

- (1) the characteristics of Snell trace mapping and its inversion (figures 3 and 4);
- (2) downward continuation in Snell trace coordinates (figures 5 and 6); and
- (3) comparisons of the Snell trace method, radial trace method, and wave equation phase methods in depth velocity variable media (figures 7 and 8).

From the details given in the figure captions we can make the following observations.

- (1) Downward continuation by transformation into Snell trace coordinates works well.
- (2) The more accurate the depth velocity function used to transform into Snell coordinates, the better the quality of the downward continuation will be. That is to also say that though downward continuation using radial trace coordinates works to a limited extent, Snell trace coordinates work better.
- (3) Being basically a ray tracing method, downward continuation in Snell trace coordinates is free of certain artifacts present in wave equation methods such as edge effects, missing data, and dispersive noise.
- (4) The Snell trace method is not without its own problems such as mapping interpolation artifacts, and misplacement of events not assumed in the Snell trace model such as refractions.

### Appendix A: Derivation of that the Downward Continuation of a Slant Stack is a P-Dependent Time Shift

First we begin with the double square root equation in slant stack coordinates.

$$\frac{dP}{dz} = -i \frac{\omega}{v} \left[ \sqrt{1 - (Y + p)^2} + \sqrt{1 - (Y - p)^2} \right] P \quad (4)$$

The wavenumber ratio  $Y = \frac{vk_y}{2\omega}$  is zero for flat events giving

$$\frac{dP}{dz} = -2i\omega \sqrt{\frac{1}{v^2} - p^2} P \quad (5)$$

Fourier transforming  $\omega$  into a time derivative and replacing  $p$  by its  $\vartheta$  expression leaves

$$\frac{dP}{dz} = \left[ -2 \frac{\cos \vartheta}{v} \right] \frac{dP}{dt} \quad (6)$$

Equation (6) is just a time shift. The total time shift is obtained by integrating the bracketed term over  $z$ .

**Appendix B: Implementation Approximation to Snell Trace Mapping**

The Snell trace mapping scheme of equations (1) and (2) require two dimensional interpolation. With the below approximation, we can reduce the interpolation to one dimension.

Differentiate equation (2) to obtain

$$dt_S = dz \frac{v}{\cos\vartheta} \quad (7)$$

Use this to change the variable of integration in equation (1) to

$$h_S = \int_0^{t_S} dt_S v \sin\vartheta \quad (8)$$

The approximation is made in how velocity is defined.

$$v(z) = v(t,p) \sim v(t)$$

This approximation becomes increasingly inaccurate for larger  $p$ , i.e. large offsets.

**REFERENCES**

- [1] Schultz, "A Method for the Direct Estimation of Interval Velocities in the Near Surface" 50th SEG preprint paper, 1980

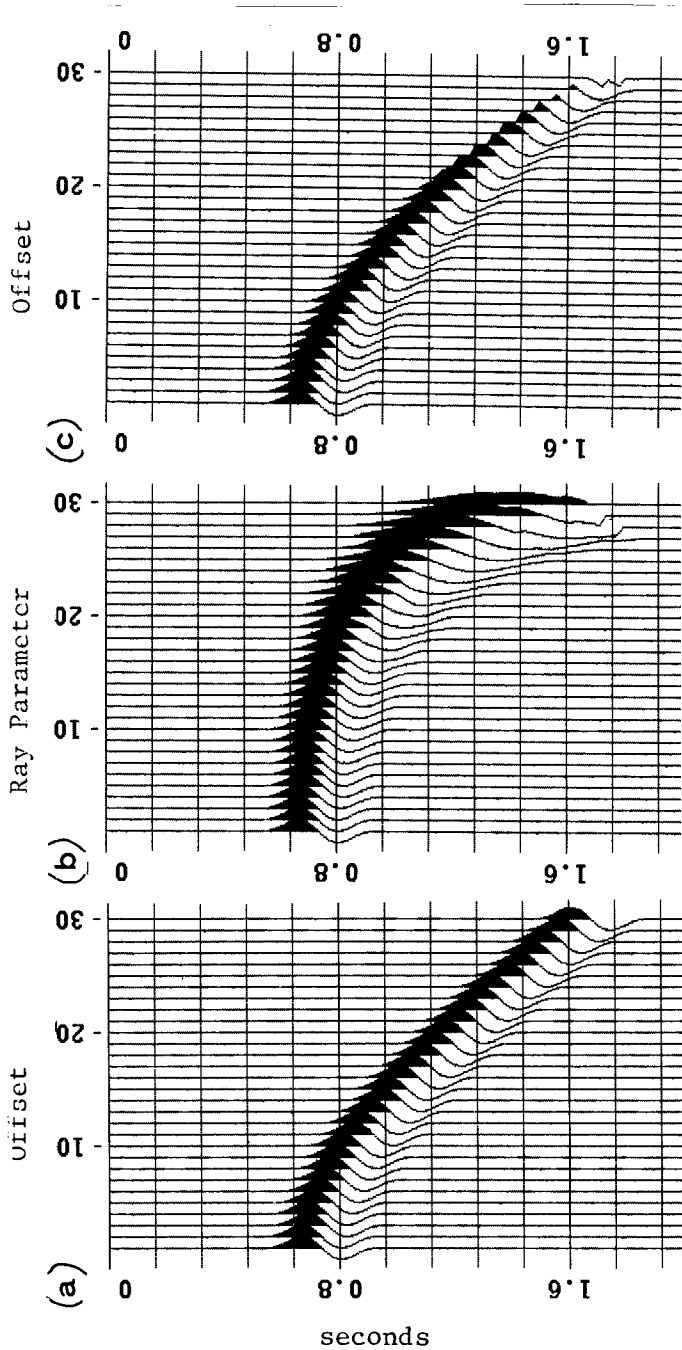


FIG. 3. This set of figures shows a mapping of a synthetic CDP gather into Snell trace coordinates and its inverse. Part (a) is the original CDP gather. It is the synthetic used in Yedlin and Thorson (this SEP report). It was generated by ray tracing with the waveform convolved on afterwards. The parameters are #offset=30 near=0.  $\Delta\text{off}=150\text{m}$  #t=100  $\Delta t=0.02\text{s}$  tfinal=2s #p=30 firstp=0.  $\Delta p=1.0\text{e-}5\text{s/m}$ . event=7s eventvel=1500m/s. The event velocity was assumed for the entire depth giving straight line trajectories. The range of Snell parameters was chosen to be evenly distributed between the highest and lowest positive dips present on the CDP gather. Mapping interpolation was done along the coordinate directions. The jagged edges at high Snell values are due to inadequate mapping interpolation. Part (c) is the Snell trace gather of part (a) mapped back into CDP coordinates. Differences between part (c) and part (a) are also due to interpolation.

The mapping interpolation should be done along the time dip of an event for better results. (See Hale SEP-25.) Fortunately, it is easy to determine the time dip of event during Snell trace mapping. According to the geometry of figure 2, the time dip of a reflector segment is the Snell parameter of the Snell trace trajectory passing through it.

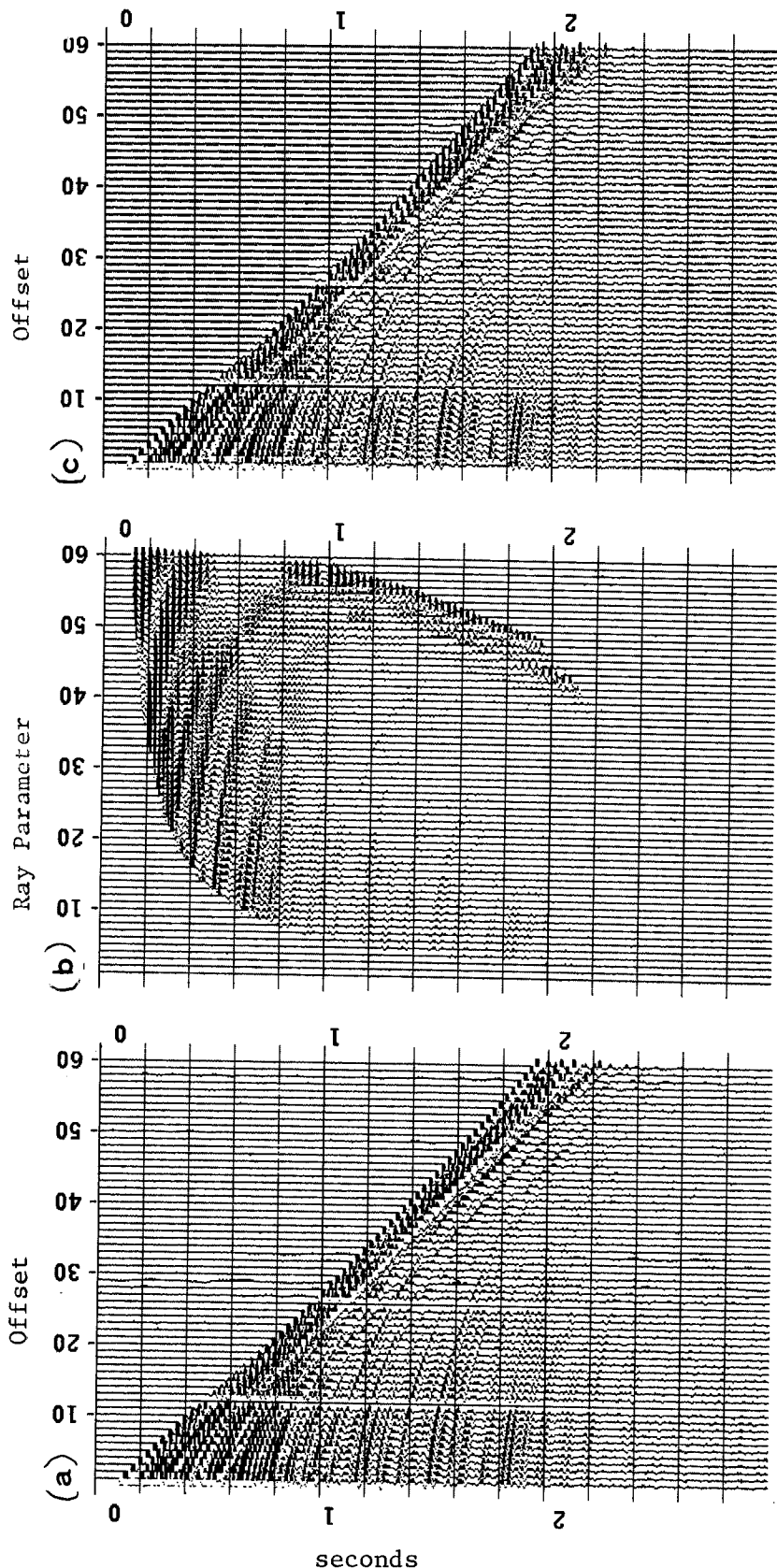


FIG. 4. This set of figures shows the mapping of a real CDP gather into Snell trace coordinates and its inverse. This gather is from a Conoco dataset used by Clayton et al (this SEP report). The parameters to this dataset are those used in figure 1. The distribution of Snell parameters here is  $\#p=60$   $p1=0$ .  $\Delta p=.0087\text{km/s}$ . The distribution of Snell parameters was chosen to be evenly divided between the highest and lowest time dips of the reflectors. Part (a) is original gather, part (b) is its mapping into Snell trace coordinates, and part (c) is the inversion back into offset coordinates. A little fidelity is lost in the upper, wide offset traces on part (c), but is virtually unobservable.

The features of the Snell trace gather in part (b) are explained in Ottolini's SEP-20 report, but here is a brief review. The two dead traces on the original gather appear as arched gaps in the Snell trace gather giving clues as to the mapping. The the sharp upper left cut-off is due to the missing inner offsets on the original gather (near=135m). In the lower right corner is the less visible cut-off due to missing wide offsets. The refraction events at the far right of part (b) actually curve back into lower Snell parameters with increasing time. This artifact is due to that the Snell trace theory is not designed for refractions.



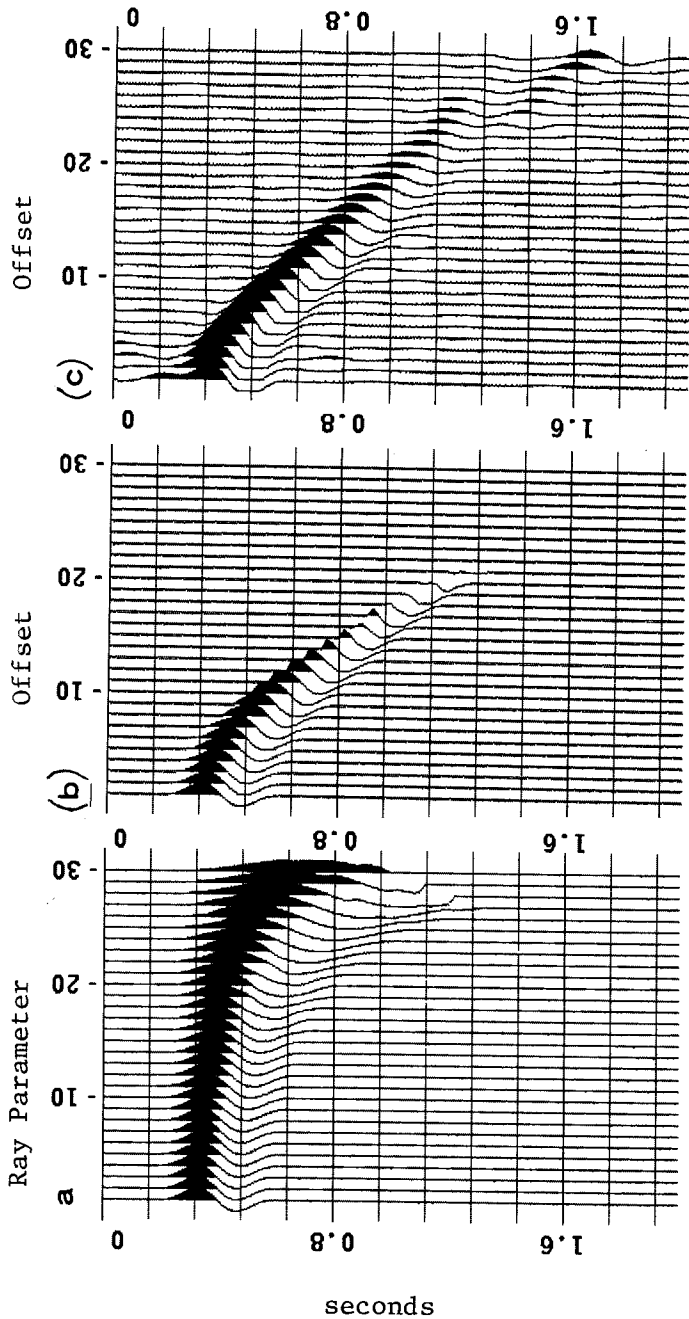


FIG. 5. This figure shows the downward continuation procedure of the synthetic CDP gather of figure 3. It is continued half way to the reflection event ( $\tau=0.34s$ ). Part (a) is the CDP gather transformed into Snell trace coordinates. A p-dependent time shift has been applied to each trace. Part (b) is the downward continued gather transformed back into offset coordinates. As expected, the hyperbola has started to collapse toward zero offset and zero travel time. Part (c) is the downward continuation to the same depth using the frequency domain phase shift wave equation method. One artifact is wraparound in the lower right due to the periodic nature of the frequency domain transformation. A second artifact is an upward curving of the tail of the hyperbola attributed to the sudden truncation of data at the edge of the gather. (Papers at the beginning of this SEP report discuss this problem.) The third artifact is noise at the apex of the hyperbola due to relatively coarse sampling of this small dataset.

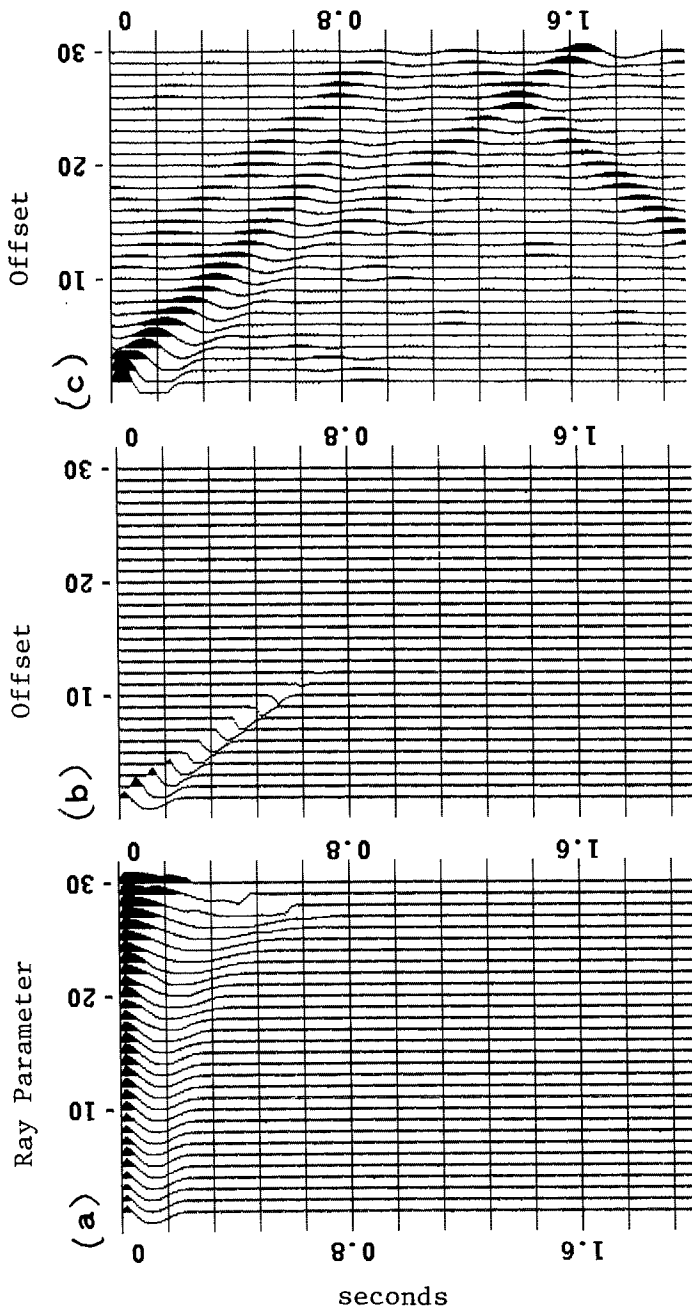


FIG. 6. This figure shows the same synthetic CDP gather of figure 3 downward continued just to the top of the reflection event. Parts (a), (b), and (c) have been processed in exactly the same way as figure 5. Part (a) is the downward continued Snell trace gather. Part (b) is the transformation of part (a) back into offset space. Part (c) is a phase-shift downward continuation. The reflection event has pretty much collapsed in part (b). The artifacts are similar to those in figure 5.

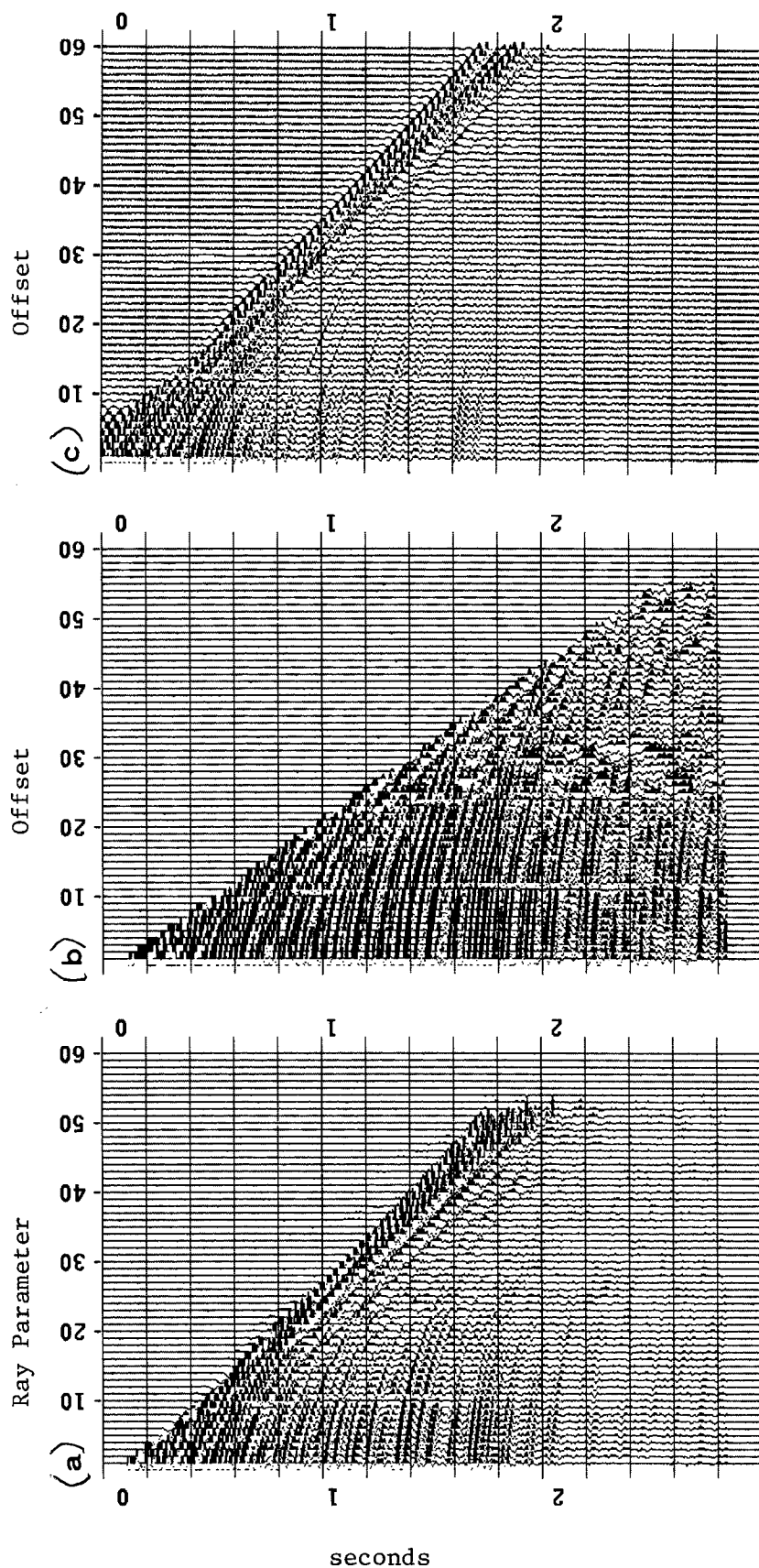


FIG. 7. This figure shows the downward continuation of the real data CDP gather of figure 4 to the seafloor ( $\tau=1.5s$ ). Three different downward continuation methods are used. Part (a) is the result through a Snell trace coordinate transformation. Part (b) is the result through a radial trace coordinate transformation. Equation (3) was used to compute the radial trace trajectories using the same Snell parameters as for part (a) and the water velocity. All three methods exhibit the collapsing hyperbola of downward continuation. As indicated by the leftward curvature of the two dead traces, the shallower events correctly collapse faster than the deeper events. The quality of the radial trace continuation of part (b) degrades at wide offsets. The phase shift downward continuation of part (c) has noise at low times.

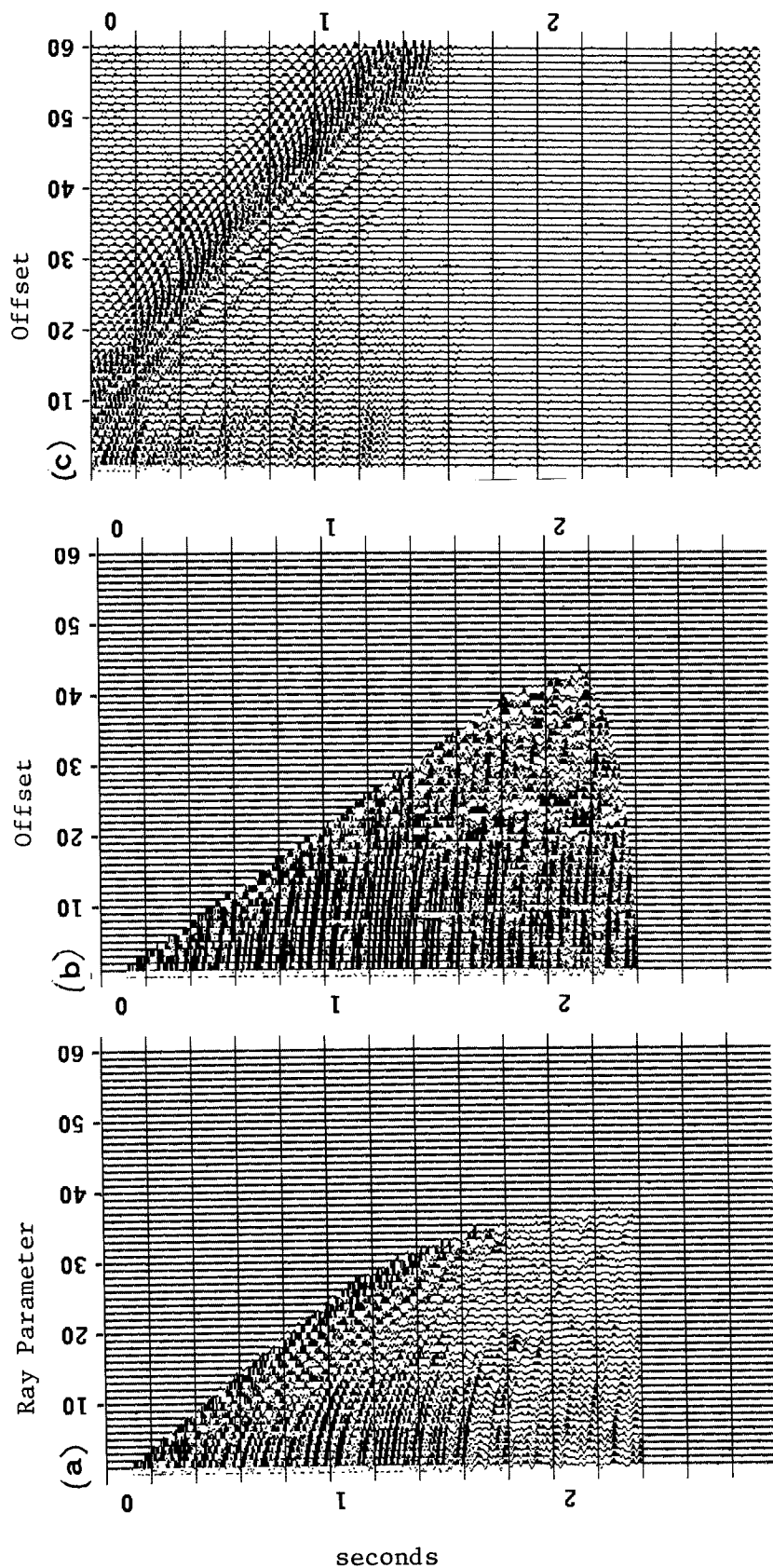


FIG. 8. This figure shows same processing as in the previous figure, but continued deeper to shift methods. The basic nature of the collapsing hyperbolas is preserved in the Snell trace method of part (a). However, the refraction events did not fare as well. In the radial trace result of part (b) both the reflections and refractions suffer. The radial trace method is modestly successful, but is not as good as the Snell trace theory which takes depth velocity variation into account. On the phase shift result in part (c) the artifacts have become worse.